



OPEN

The flexible linker of the secreted FliK ruler is required for export switching of the flagellar protein export apparatus

Miki Kinoshita¹, Seina Tanaka², Yumi Inoue^{1,5}, Keiichi Namba ^{1,3,4}, Shin-Ichi Aizawa² & Tohru Minamino ^{1*}

The hook length of the flagellum is controlled to about 55 nm in *Salmonella*. The flagellar type III protein export apparatus secretes FliK to determine hook length during hook assembly and changes its substrate specificity from the hook protein to the filament protein when the hook length has reached about 55 nm. *Salmonella* FliK consists of an N-terminal domain (FliK_N, residues 1–207), a C-terminal domain (FliK_C, residues 268–405) and a flexible linker (FliK_L, residues 208–267) connecting these two domains. FliK_N is a ruler to measure hook length. FliK_C binds to a transmembrane export gate protein FlhB to undergo the export switching. FliK_L not only acts as part of the ruler but also contributes to this switching event, but it remains unknown how. Here we report that FliK_L is required for efficient interaction of FliK_C with FlhB. Deletions in FliK_L not only shortened hook length according to the size of deletions but also caused a loose length control. Deletion of residues 206–265 significantly reduced the binding affinity of FliK_C for FlhB, thereby producing much longer hooks. We propose that an appropriate length of FliK_L is required for efficient interaction of FliK_C with FlhB.

The bacterial flagellar hook is a tubular structure composed of the hook protein FlgE and acts as a universal joint to smoothly transmit torque produced by the flagellar motor to the long helical filament that functions as a propeller¹. The hook length of the *Salmonella* flagellum is controlled to about 55 nm², and the length control is important for the universal joint mechanism³.

The flagellar type III protein export apparatus is located at the flagellar base and transports FlgE subunits from the cytoplasm to the distal end of the growing hook structure for hook assembly^{4,5}. Newly exported FlgE monomers polymerize onto the nascent hook structure with the help of the hook cap (FlgD), which is located at the hook tip⁶. Interactions between FlgD and FlgE suppress the leakage of FlgE subunits into the culture media so that each FlgE subunit can be efficiently incorporated into the hook structure^{7,8}.

When hook length has reached about 55 nm, the flagellar type III protein export apparatus changes its substrate specificity, thereby terminating hook assembly and initiating filament assembly^{9,10}. FliK, FlhA, FlhB and Flk are directly involved in the export switching process^{11–14}. If certain mutations in FliK, FlhB or FlhA inhibits the export switching of the flagellar type III protein export apparatus, unusually elongated hooks called polyhooks are generated. FlhA and FlhB are transmembrane proteins of the flagellar protein export apparatus^{15,16}, and their C-terminal cytoplasmic domains (FlhA_C, FlhB_C) project into the cavity within the basal body C ring^{15,16}. FlhA_C forms a homo-nonameric ring structure^{17,18} and provides binding-sites for cytoplasmic export components (FliH, FliI, FliJ)^{19–21} and flagellar export chaperones (FlgN, FliS, FliT) in with their cognate substrates^{22–25}. Interactions of FlhA_C with FliH, FliI and FliJ seems to support the strict order of flagellar assembly^{26,27}. The interaction of FlhB_C with FliK induces the export switching of the flagellar type III protein export apparatus^{28–30}. FlhB_C binds to FliH, FliI, FliJ and export substrates such as FlgD and FlgE^{19,31,32}. Conformational changes of FlhA_C and FlhB_C

¹Graduate School of Frontier Biosciences, Osaka University, 1-3 Yamadaoka, Suita, Osaka, 565-0871, Japan.

²Department of Life Sciences, Prefectural University of Hiroshima, 562 Nanatsuka, Shobara, Hiroshima, 727-0023, Japan. ³RIKEN Spring-8 Center and Center for Biosystems Dynamics Research, 1-3 Yamadaoka, Suita, Osaka, 565-0871, Japan. ⁴JEOL YOKOGUSHI Research Alliance Laboratories, Osaka University, 1-3 Yamadaoka, Suita, Osaka, 565-0871, Japan. ⁵Present address: Department of Ophthalmology and Visual Sciences, Kyoto University Graduate School of Medicine, Kyoto, 606-8507, Japan. *email: tohru@fbs.osaka-u.ac.jp

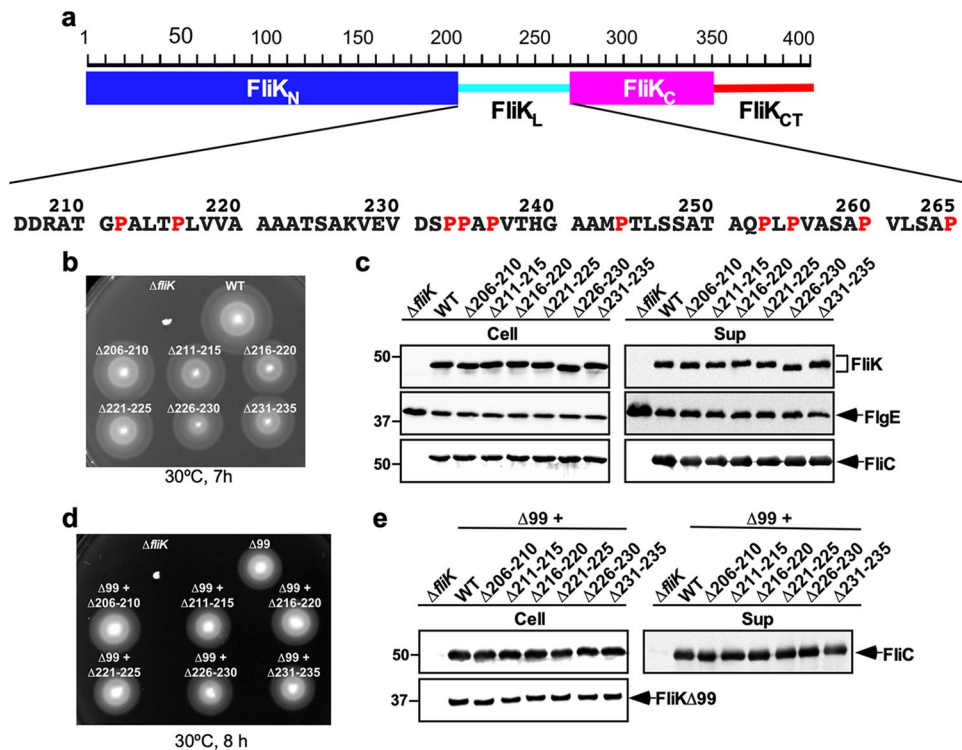


Figure 1. Effect of deletions of five residues within the N-terminal region of FliK_L on FliK function. (a) Domain organization of FliK ruler. FliK consists of the N-terminal ruler domain (FliK_N), the C-terminal export switch domain (FliK_C) and a flexible linker (FliK_L) connecting these two domains. FliK_C has an intrinsically disordered C-terminal tail (FliK_{CT}). Amino acid sequence of FliK_L is shown. Proline residues are highlighted in red. (b) Motility of TH8426 harboring pTrc99AFF4 ($\Delta fliK$), pMK002 (WT), pMMK1001 ($\Delta 206-210$), pMMK1002 ($\Delta 211-215$), pMMK1003 ($\Delta 216-220$), pMMK1004 ($\Delta 221-225$), pMMK1005 ($\Delta 226-230$) or pMMK1006 ($\Delta 231-235$) in 0.35% soft agar. Plates were incubated at 30°C for 7 hours. (c) Secretion assays of FliK, FlgE and FliC. Immunoblotting using polyclonal anti-FliK (1st row), anti-FlgE (2nd row) or anti-FliC (3rd row) antibody, of whole cell proteins (Cell) and culture supernatants (Sup) from the above strains. The regions of interest were cropped from original immunoblots shown in Fig. S6a in the Supplemental information using a software, Photoshop CS6, and then the contrast and brightness were adjusted. The positions of molecular mass markers (kDa) are indicated on the left. (d) Motility of TH8426 harboring pTrc99AFF4 ($\Delta fliK$), pNM201 ($\Delta 99$), pMMK1016 ($\Delta 99 + \Delta 206-210$), pMMK1017 ($\Delta 99 + \Delta 211-215$), pMMK1018 ($\Delta 99 + \Delta 216-220$), pMMK1019 ($\Delta 99 + \Delta 221-225$), pMMK1020 ($\Delta 99 + \Delta 226-230$) or pMMK1021 ($\Delta 99 + \Delta 231-235$) in 0.35% soft agar containing 1 mM IPTG. Plates were incubated at 30°C for 8 hours. (e) Secretion assay of FliC. Immunoblotting using polyclonal anti-FliC (1st row) or anti-FliK (2nd row) antibody, of whole cell proteins (Cell) and culture supernatants (Sup) from the above strains. The regions of interest were cropped from original immunoblots shown in Fig. S6b using Photoshop CS6, and then the contrast and brightness were adjusted.

are required for the substrate specificity switching of the flagellar protein export apparatus upon hook completion^{18,28,33}. Flk interferes with premature switching of the protein export apparatus during hook-basal body assembly^{13,14,34}.

The flagellar type III protein export apparatus transports several FliK molecules during hook assembly to determine hook length in a way that the protein export apparatus switches its substrate specificity when the hook length has reached about 55 nm³⁵⁻³⁸. *Salmonella* FliK is a 405 amino-acid protein consisting of the N-terminal ruler domain (FliK_N, residues 1–207), the C-terminal export switch domain (FliK_C, residues 268–405) and a flexible linker (FliK_L, residues 208–267) connecting these two domains (Fig. 1a)³⁹⁻⁴¹. FliK_N contains a hook-type export signal recognized by the flagellar type III protein export apparatus^{31,35}. Insertions and deletions in FliK_N make the hook longer and shorter, respectively, suggesting that FliK_N is a molecular ruler⁴². FliK_N binds to FlgD and FlgE⁴³⁻⁴⁵, and deletion of residues 129–159 in FliK_N reduces the binding affinity of FliK for FlgE, thereby producing longer hooks with the filament attached. This suggests that the interaction of FliK_N with FlgE is required for proper hook length measurement⁴⁴. FliK_C consists of a compactly folded core domain consisting of residues 268–352 and an intrinsically disordered C-terminal tail composed of residues 353–405 (FliK_{CT}) (Fig. 1a)^{40,46}. The core domain of FliK_C binds to FlhB_C to allow the flagellar protein export apparatus to switch its substrate specificity from rod- (FlgB, FlgC, FlgF, FlgG, FlgJ, FlgE) and hook-type (FlgD, FlgE, FliK) to filament-type (FlgK, FlgL, FlgM, FliC, FlgD)^{11,12,28,45,47}. Genetic analyses of FliK_{CT} have suggested that FliK_{CT} controls the export switching activity of FliK_C during hook assembly^{45,47}.

FliK_L contains ten proline residues (Fig. 1a)³⁹ and hence is intrinsically disordered⁴¹. Hook lengths of the *Salmonella fliK*(Δ238–269) (32 residues deletion) and *fliK*(Δ248–269) (22 residues deletion) mutants are 40.2 ± 6.1 nm [mean ± standard deviation (SD)] and 51.0 ± 8.8 nm, where their average lengths are shorter than that of the wild-type strain (52.7 ± 4.5 nm)⁴². The length of the hook produced by the *fliK*(Δ161–216) mutant (56 residues deletion) is 48.7 ± 22.3 nm, where the average is also shorter than that of the wild-type strain by 4 nm. However, the SD value is larger than the wild-type one, indicating a much looser length control of the hook structure⁴². Furthermore, deletions of residues 161–223 and 161–244 cause polyhooks without the filament attached whereas a deletion of residues 208–269 results in the polyhooks with the filament attached (polyhook–filament phenotype)⁴². These observations raise the possibility that FliK_L not only acts as part of the ruler but also contributes to substrate specificity switching of the flagellar protein export apparatus. To clarify this hypothesis, we constructed a series of mutant variants of FliK with in-frame deletions within FliK_L. We show that a proper length of FliK_L between FliK_N and FliK_C is required for efficient interaction of FliK_C with FlhB_C.

Results

Effect of deletions of five amino-acid residues within residues 206–235 on hook length control.

It has been shown that the N-terminal portion of FliK_L is responsible for proper measurement of hook length⁴². To clarify the role of residues 206–235 of FliK_L in the hook length control, we constructed a series of mutant variants of FliK with sequential 5-amino-acid deletions within a region of residues 206–235, namely FliK(Δ206–210), FliK(Δ211–215), FliK(Δ216–220), (Δ221–225), (Δ226–230) and FliK(Δ231–235) (Table 1). These six *fliK* deletion variants fully restored motility of the Δ*fliK* mutant in 0.35% soft agar plates when they were expressed from the pTrc99A-based plasmid (Fig. 1b). Consistently, the levels of FlgE and FliC secreted by these deletion mutants were detected at the wild-type levels (Fig. 1c, 2nd and 3rd rows). These *fliK* deletions did not affect either protein stability or protein secretion into the culture media (Fig. 1c, 1st row). Therefore, we conclude that these in-frame deletions do not affect FliK function at all.

The length of the most extended polypeptide chain is 0.37 nm per residue. If FliK_L adopts a fully extended conformation to act as part of the ruler, we predicted that these 5-amino-acid deletions within residues 206–235 of FliK_L would reduce the hook length by 1.9 nm. Therefore, we measured the hook length of these *fliK* deletion mutants. The average hook length of the *fliK*(Δ206–210), *fliK*(Δ211–215), *fliK*(Δ216–220), *fliK*(Δ221–225), *fliK*(Δ226–230) and *fliK*(Δ231–235) mutants were 48.5 ± 4.5 nm (n = 113), 49.3 ± 5.2 nm (n = 168), 49.0 ± 5.6 nm (n = 130), 48.6 ± 4.2 nm (n = 118), 49.2 ± 4.2 nm (n = 232) and 49.6 ± 5.4 nm (n = 126), respectively, which were shorter than the length of the wild-type hook (53.3 ± 6.5 nm, n = 154) (Fig. S1). Over-expression of FliK slightly shortens the hook length. In contrast, when the expression level of FliK is reduced, the cell produces polyhooks, sometimes with the filament attached^{27,48}. Polyhooks are frequently observed when FlgE is overproduced in wild-type cells^{27,43}. Thus, the balance between the secretion levels of FlgE and FliK seems to be critical for the proper termination of the hook assembly. Since 5-amino-acid deletions within residues 206–235 shorten the hook length by 4 nm, which is shorter than the predicted value, we assume that these deletions may affect not only hook length measurements but also the secretion process of FliK by the type III protein export apparatus and/or the export switching process of the protein export apparatus induced by the interaction of FliK_C with FlhB_C.

To directly test if these 5 amino-acid deletions affect the interaction of FliK_C with FlhB_C, it is necessary to analyze the protein transport process of FliK and the export switching process of the flagellar type III protein export apparatus separately. To do so, we used a *fliK*(Δ2–99) allele, which is an export deficient variant of FliK, because it retains the ability to catalyze export switching of the flagellar type III protein export apparatus when over-expressed⁴⁹. We introduced deletions of residues 206–210, 211–215, 216–220, 221–225, 226–230 or 231–235 into the *fliK*(Δ2–99) allele by inverse PCR method and analyzed motility of the Δ*fliK* mutant cells over-expressing FliK(Δ2–99) with these deletions in the presence of 1 mM isopropyl β-D-1-thiogalactopyranoside (IPTG). These additional deletions did not affect motility of the cells over-expressing FliK(Δ2–99) (Fig. 1d). Consistently, the inner and extra-cellular amounts of FliC seen in the *fliK*(Δ2–99 + Δ206–210), *fliK*(Δ2–99 + Δ211–215), *fliK*(Δ2–99 + Δ216–220), *fliK*(Δ2–99 + Δ221–225), *fliK*(Δ2–99 + Δ226–230) and *fliK*(Δ2–99 + Δ231–235) cells were the same as those in the *fliK*(Δ2–99) cells (Fig. 1e, 1st row). Since these deletions did not affect the expression level of FliK(Δ2–99) (Fig. 1e, 2nd row), we suggest that they do not affect the interaction of FliK(Δ2–99) with FlhB_C. Therefore, we propose that these deletions may affect the protein transport process of FliK as well as hook length measurement.

To further understand the ruler function of residues 206–235 in FliK_L, we constructed larger deletion variants, FliK(Δ206–215), FliK(Δ216–225), FliK(Δ226–235), FliK(Δ206–220), FliK(Δ221–235) and FliK(Δ206–235) and analyzed their motility in 0.35% soft agar plates (Fig. S2a). Motility of the *fliK*(Δ206–215), *fliK*(Δ226–235), *fliK*(Δ206–220), *fliK*(Δ221–235) and *fliK*(Δ206–235) cells was almost the same as wild-type motility whereas that of the *fliK*(Δ216–225) mutant was slightly less than the wild-type level (Fig. S2a). The cellular and secretion levels of these deletion variants were essentially the same as the wild-type levels (Fig. S2b). Because these deletion mutants were expressed from the pTrc99A/F4 vector, it is also possible that their over-expression results in motility comparable to the wild-type level. To verify this possibility, the wild-type *fliK* allele on the chromosomal DNA was replaced by the *fliK*(Δ206–235) allele. Motility of the *fliK*(Δ206–235) mutant was slightly less than that of wild-type cells (Fig. S2c). To test whether the deletion of residues 206–235 affect hook length, we isolated hook-basal bodies from the *fliK*(Δ206–235) mutant and measured the hook length (Figs. 2 and S3). A major peak of the hook length distribution was shifted to a shorter value than that of the wild-type (Fig. 2). While the majority of wild-type hook length was distributed within a range from 50 nm to 60 nm, the hook length distribution of the *fliK*(Δ206–235) mutant showed a major peak population between 41 nm and 50 nm. However, longer hooks were also observed albeit shorter than those of polyhooks produced by the Δ*fliK* mutant [362.8 ± 200.9 nm (N = 146)]. As a result, the average hook length of the *fliK*(Δ206–235) mutant was 54.5 ± 15.5 nm (n = 112), compared to 53.8 ± 5.6 nm (n = 130) for the wild-type. The SD value of the *fliK*(Δ206–235) mutant was larger than the wild-type one, indicating that the deletion of residues 206–235 in FliK_L cause a looser hook length control

Strains and Plasmids	Relevant characteristics	Source or reference
<i>E. coli</i>		
BL21 Star (DE3)	Overexpression of proteins	Novagen
<i>Salmonella</i>		
SJW1103	Wild type for motility and chemotaxis	61
TH8426	$\Delta fliK$	47
MMK1012	<i>fliK</i> ($\Delta 206-235$)	This study
MMK1013	<i>fliK</i> ($\Delta 206-245$)	This study
MMK1014	<i>fliK</i> ($\Delta 206-255$)	This study
MMK1015	<i>fliK</i> ($\Delta 206-265$)	This study
Plasmids		
pTrc99AFF4	Modified pTrc expression vector	62
pKM002	pTrc99AFF4/ <i>FliK</i>	48
pNM201	pTrc99AFF4/ <i>FliK</i> ($\Delta 2-99$)	44
pMMK521	pETDuet-1/ <i>FliK</i> (I304amber) + FlhB _C	45
pMMK1001	pTrc99AFF4/ <i>FliK</i> ($\Delta 206-210$)	This study
pMMK1002	pTrc99AFF4/ <i>FliK</i> ($\Delta 211-215$)	This study
pMMK1003	pTrc99AFF4/ <i>FliK</i> ($\Delta 216-220$)	This study
pMMK1004	pTrc99AFF4/ <i>FliK</i> ($\Delta 221-225$)	This study
pMMK1005	pTrc99AFF4/ <i>FliK</i> ($\Delta 226-230$)	This study
pMMK1006	pTrc99AFF4/ <i>FliK</i> ($\Delta 231-235$)	This study
pMMK1007	pTrc99AFF4/ <i>FliK</i> ($\Delta 206-215$)	This study
pMMK1008	pTrc99AFF4/ <i>FliK</i> ($\Delta 216-225$)	This study
pMMK1009	pTrc99AFF4/ <i>FliK</i> ($\Delta 226-235$)	This study
pMMK1010	pTrc99AFF4/ <i>FliK</i> ($\Delta 206-220$)	This study
pMMK1011	pTrc99AFF4/ <i>FliK</i> ($\Delta 221-235$)	This study
pMMK1012	pTrc99AFF4/ <i>FliK</i> ($\Delta 206-235$)	This study
pMMK1013	pTrc99AFF4/ <i>FliK</i> ($\Delta 206-245$)	This study
pMMK1014	pTrc99AFF4/ <i>FliK</i> ($\Delta 206-255$)	This study
pMMK1015	pTrc99AFF4/ <i>FliK</i> ($\Delta 206-265$)	This study
pMMK1015SP	pTrc99AFF4/ <i>FliK</i> ($\Delta 206-265SP$)	This study
pMMK1016	pTrc99AFF4/ <i>FliK</i> ($\Delta 2-99 + \Delta 206-210$)	This study
pMMK1017	pTrc99AFF4/ <i>FliK</i> ($\Delta 2-99 + \Delta 211-215$)	This study
pMMK1018	pTrc99AFF4/ <i>FliK</i> ($\Delta 2-99 + \Delta 216-220$)	This study
pMMK1019	pTrc99AFF4/ <i>FliK</i> ($\Delta 2-99 + \Delta 221-225$)	This study
pMMK1020	pTrc99AFF4/ <i>FliK</i> ($\Delta 2-99 + \Delta 226-230$)	This study
pMMK1021	pTrc99AFF4/ <i>FliK</i> ($\Delta 2-99 + \Delta 231-235$)	This study
pMMK1022	pTrc99AFF4/ <i>FliK</i> ($\Delta 2-99 + \Delta 206-215$)	This study
pMMK1023	pTrc99AFF4/ <i>FliK</i> ($\Delta 2-99 + \Delta 216-225$)	This study
pMMK1024	pTrc99AFF4/ <i>FliK</i> ($\Delta 2-99 + \Delta 226-235$)	This study
pMMK1025	pTrc99AFF4/ <i>FliK</i> ($\Delta 2-99 + \Delta 206-220$)	This study
pMMK1026	pTrc99AFF4/ <i>FliK</i> ($\Delta 2-99 + \Delta 221-235$)	This study
pMMK1027	pTrc99AFF4/ <i>FliK</i> ($\Delta 2-99 + \Delta 206-235$)	This study
pMMK1028	pTrc99AFF4/ <i>FliK</i> ($\Delta 2-99 + \Delta 206-245$)	This study
pMMK1029	pTrc99AFF4/ <i>FliK</i> ($\Delta 2-99 + \Delta 206-255$)	This study
pMMK1030	pTrc99AFF4/ <i>FliK</i> ($\Delta 2-99 + \Delta 206-265$)	This study
pMMK1030SP	pTrc99AFF4/ <i>FliK</i> ($\Delta 2-99 + \Delta 206-265SP$)	This study
pMMK1031	pETDuet-1/ <i>FliK</i> ($\Delta 2-99 + I304amber$) + FlhB _C	This study
pMMK1032	pETDuet-1/ <i>FliK</i> ($\Delta 2-99 + \Delta 206-265 + I304amber$) + FlhB _C	This study
pMMK1032SP	pETDuet-1/ <i>FliK</i> ($\Delta 2-99 + \Delta 206-265SP + I304amber$) + FlhB _C	This study

Table 1. Strains and plasmids used in this study.

than the wild-type. Therefore, we suggest that a deletion of residues 206–235 not only shortens the hook length according to the size of deletion but also affects the interaction of *FliK_C* with *FlhB_C* during hook assembly.

Effect of much larger deletions within *FliK_L* on hook length control and substrate specificity switching. To clarify the role of *FliK_L* in the export switching process of the flagellar type III protein export apparatus, the wild-type *fliK* allele on the chromosome was replaced by the *fliK*($\Delta 206-245$), *fliK*($\Delta 206-255$) or

fliK(Δ 206–265) allele. Motility of these mutants were worse than wild-type motility (Fig. 3a) although the cellular and secreted amounts of FlgE and FliC were detected almost at the wild-type levels (Fig. 3b, 2nd and 3rd rows). Because neither cellular nor extracellular FliK level was affected by these larger deletions within FliK_L (Fig. 3b, 1st row), this suggests that these deletions reduce FliK function.

To test whether these larger deletions affect the hook length control, we measured the hook length of the *fliK*(Δ 206–245), *fliK*(Δ 206–255) and *fliK*(Δ 206–265) mutants (Figs. 3c and S3). The hook length distribution of the *fliK*(Δ 206–245) mutant shows a major peak population between 45 nm and 55 nm. Longer hooks and polyhooks were seen for the *fliK*(Δ 206–255) and *fliK*(Δ 206–265) mutants although shorter hooks were also observed (Fig. S3). As a result, the average hook lengths of the *fliK*(Δ 206–245), *fliK*(Δ 206–255) and *fliK*(Δ 206–265) mutants were 54.4 ± 17.6 nm ($n = 226$), 75.0 ± 38.9 nm ($n = 160$) and 107.1 ± 65.0 nm ($n = 300$), respectively, indicating that the hook length control becomes worse in the *fliK*(Δ 206–255) and *fliK*(Δ 206–265) mutants.

To investigate whether these larger deletions directly affect the export switching function of FliK_C, we introduces deletions residues 206–245, 206–255 or 206–265 into the *fliK*(Δ 2–99) allele. Motility of the cells over-expressing FliK(Δ 2–99) with these three deletions was reduced significantly (Fig. 3d), and especially the deletion of residues 206–265 reduced the cellular and extracellular levels of FliC by about 3-fold, thereby reducing motility considerably (Fig. 3e). This suggests that these three deletions reduce the export switching function of FliK_C.

To clarify why the deletion of residues 206–265 considerably reduces the export switching activity of FliK_C, we isolated fourteen pseudorevertants from the cells over-expressing FliK(Δ 2–99) with an in-frame deletion of residues 206–265. Motility of these pseudorevertants was much better than that of its parent cells and was slightly better than that of the cells over-expressing FliK(Δ 2–99) (Fig. 4a). Consistently, the cellular and extracellular levels of FliC seen in these pseudorevertants were much higher than those in the *fliK*(Δ 2–99 + Δ 206–265) cells and slightly larger than those in the *fliK*(Δ 2–99) cells (Fig. 4b). These results indicate that the suppressor mutations enhance the probability of export switching to occur. DNA sequence analysis revealed that all suppressor mutations are insertion mutation of a DNA fragment encoding 100 amino-acid residues corresponding to residues 111–270 without residues 206–265 due to gene duplication (Fig. 4c). As a result, this intragenic FliK(Δ 2–99 + Δ 206–265) suppressor mutation variant, namely FliK(Δ 2–99 + Δ 206–265SP), showed much slower mobility on SDS-PAGE than FliK(Δ 2–99) and FliK(Δ 2–99 + Δ 206–265) (Fig. 4b). The inserted sequence of the suppressor mutant was located between Glu-270 and Trp-271 residues in helix α 1 of the core domain of FliK_C (Fig. 4d). The *fliK*(Δ 2–99 + Δ 206–265) mutant cells produced polyhooks sometimes with filaments attached (Fig. S4). In contrast, most of the pseudorevertant cells had a few flagella (Fig. S4). The pseudorevertant cells produced normal hooks or much shorter polyhooks compared to the *fliK*(Δ 2–99) and *fliK*(Δ 2–99 + Δ 206–265) cells (Fig. S4). Careful measurements of the hook length indicated that the average hook length of the pseudorevertant were 113.4 ± 136.7 nm ($n = 308$), compared to 194.5 ± 180.4 nm ($n = 308$) for the *fliK*(Δ 2–99) cells and 503.1 ± 281.3 nm ($n = 301$) for the *fliK*(Δ 2–99 + Δ 206–265) cells (Figs. 5 and S5). These results led to a conclusion that FliK_L is required for efficient substrate specificity switching of the flagellar type III protein export apparatus.

Interaction between FliK(Δ 2–99) and FlhB_C. Targeted photo-crosslinking experiments have shown that Val-302 and Ile-304 of FliK_C are in relatively close proximity of FlhB_C, allowing FliK to form a photo-crosslinked product with FlhB_C⁴⁵. To investigate whether the deletion of residues 206–265 of FliK_L and its suppressor insertion mutation reduces and increases the binding affinity of FliK_C for FlhB_C, respectively, we introduced an amber mutation at position 304 of FliK(Δ 2–99), FliK(Δ 2–99 + Δ 206–265) and FliK(Δ 2–99 + Δ 206–265SP) to incorporate *p*-benzoyl-phenylalanine (pBPA), which is a photo-reactive phenylalanine and carried out photo-crosslinking experiments. We used FliK(I304amber) as a positive control. FliK(I304pBPA) produced a ca. 53 kDa photo-crosslinked product with FlhB_C after UV irradiation (Fig. 4e, lane 2), in agreement with a previous report⁴⁵. However, FliK(Δ 2–99 + I304pBPA) did not form any photo-crosslinked products with FlhB_C (Fig. 4e, lane 4), indicating that the binding affinity of FliK(Δ 2–99) for FlhB_C is lower than that of wild-type FliK. FliK(Δ 2–99 + Δ 206–265SP + I304pBPA) reproducibly formed a 51 kDa photo-crosslinked product along with FlhB_C (Fig. 4e, lane 8) whereas FliK(Δ 2–99 + Δ 206–265 + I304pBPA) did not (lane 6). This suggests that the inserted sequence of the pseudorevertant increases the binding affinity of FliK(Δ 2–99) for FlhB_C so that the export switching of the type III protein export apparatus occurs more efficiently.

Effect of the 100 residues suppressor insertion on the length of hook produced by the *fliK*(Δ 206–265) mutant. To investigate whether the insertion mutation of the *fliK*(Δ 2–99 + Δ 206–265) suppressor mutant also improves the export switching function of the *fliK*(Δ 206–265) mutant, we introduced the extra 100 amino-acid insertion sequence of the *fliK*(Δ 2–99 + Δ 206–265SP) mutant into the *fliK*(Δ 206–265) allele by the overlap PCR method to generate the *fliK*(Δ 206–265SP) allele. Motility of the Δ *fliK* mutant harboring pMMK1015SP [FliK(Δ 206–265SP)] was better than that of the Δ *fliK* mutant harboring pMMK1015 [FliK(Δ 206–265)] although it was worse than that of the Δ *fliK* mutant transformed with pKM002 (wild-type FliK) (Fig. 6a). Neither cellular nor extracellular FliK level was affected by the inserted sequence (Fig. 6b, 1st row). The amounts of FlgE secreted by the *fliK*(Δ 206–265SP) mutant were slightly less than that by the *fliK*(Δ 206–265) mutant and almost the same as the wild-type level (Fig. 6b, 2nd and 3rd rows). There was no difference in the cellular and extracellular FliC levels between the *fliK*(Δ 206–265) and *fliK*(Δ 206–265SP) mutants. These results indicates that the inserted sequence of the *fliK*(Δ 2–99 + Δ 206–265) suppressor mutant is also capable of improving the export switching function of FliK(Δ 206–265).

The amino acid sequence of FliK(Δ 206–265SP) is longer by 40 amino-acids than that of wild-type FliK, from which the average hook length is predicted to be about 70 nm, thereby reducing motility. To verify this hypothesis, we isolated hook-basal bodies from the Δ *fliK* mutant carrying pMMK1015 [FliK(Δ 206–265)] or pMMK1015SP

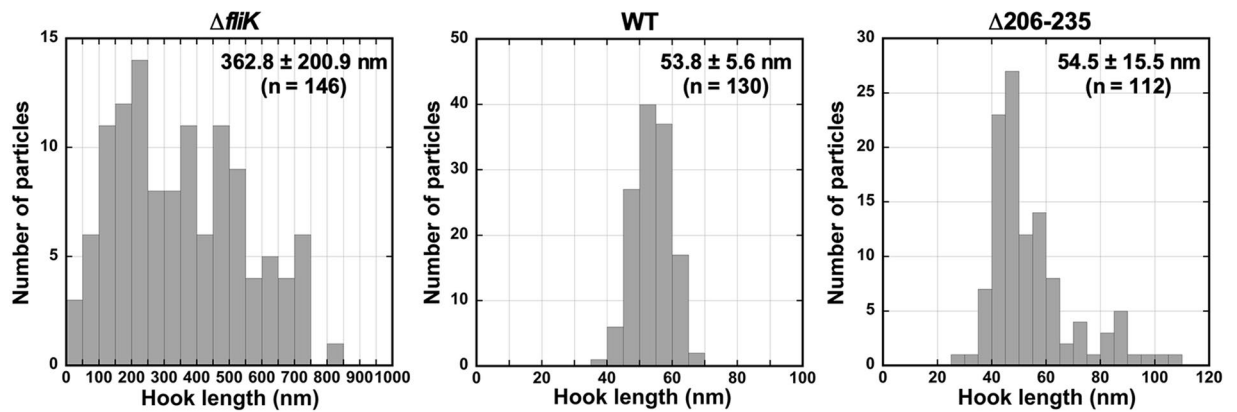


Figure 2. Effect of deletion of residues 206–235 of FliK_L on hook length control. Histograms of hook length distribution of TH8426 ($\Delta fliK$), SJW1103 (WT) and MMK1012 ($\Delta 206-235$).

[FliK($\Delta 206-265$ SP)] and measured their hook length (Figs. 6c and S5). The average hook length of the $\Delta fliK$ mutant carrying pMMK1015 was 225.4 ± 167.7 nm ($n = 127$), which were longer than that of the MMK1015 strain (107.1 ± 65.0 nm). Since FliK($\Delta 206-265$) was expressed from the pTrc99AFF4 vector, we assume that such a length difference may be a consequence of the multicopy effect of FliK($\Delta 206-265$ SP). The hook length distribution of the $\Delta fliK$ mutant carrying pMMK1015SP showed a major peak population between 61 nm and 100 nm, but much longer hooks and polyhooks were observed as well. As a result, the average hook length of the $\Delta fliK$ mutant carrying pMMK1015SP was 204.0 ± 183.9 nm ($n = 518$), which was shorter than that of the $\Delta fliK$ mutant carrying pMMK1015. This suggests that the suppressor insertion mutation increases the probability of the interaction between FliK_C with a deletion of residue 206–265 and FlhB_C, thereby increasing the export switching probability of the flagellar type III protein export apparatus.

Discussion

The bacterial injectisome directly transports virulence effector proteins into the cytosol of host cells for bacterial infection. The injectisome consists of basal body rings and a tubular structure called the needle and looks similar to the flagellar hook-basal body⁵⁰. The injectisome uses a secreted molecular ruler, SctP (originally referred to as YscP and InvJ in the *Yersinia* and *Salmonella* injectisomes, respectively) to determine the needle length in a way similar to FliK_C^{51,52}. The core domain of FliK_C is conserved among FliK/SctP family⁵³ and possesses a fold similar to the C-terminal domain of SctP of the injectisome of *Pseudomonas aeruginosa*⁵⁴. It has been shown that residues 301–350 of FliK_C are directly involved in substrate specificity switching of the flagellar type III protein export apparatus⁴⁷. Recent photo-crosslinking experiments have demonstrated that the conserved core domain of FliK_C directly binds to FlhB_C⁴⁵. Similar protein-protein interactions have been observed in the injectisome⁵⁵. These suggest that length control and substrate specificity switching mechanisms are conserved in both flagellar and injectisome systems. However, it remains unknown how the length measurement process by the secreted ruler is linked to the substrate specificity switching process of the type III protein export apparatus.

It has been reported that FliK_L forms part of the ruler to determine hook length, but a deletion of residues 208–269 results in polyhooks with the filament attached⁴², having led to a hypothesis that residues 208–235 may contribute to efficient substrate specificity switching of the flagellar type III protein export apparatus. To verify this hypothesis, we introduced systematic deletions into FliK_L and found that a deletion of residues 206–235 not only shortened hook length according to the size of deletion but also caused a loose hook length control (Fig. 2). The hook length control became much worse in the $fliK(\Delta 206-255)$ and $fliK(\Delta 206-265)$ mutants (Fig. 3c). The deletion of residues 206–265 considerably reduced the export switching function of FliK_C (Fig. 3d,e). An insertion of 100 amino-acids between Glu-270 and Trp-271 residues in the core domain of FliK_C considerably improved the switching function of FliK($\Delta 2-99 + \Delta 206-265$), thereby shortening the hook length considerably and increasing the probability of filament formation significantly (Figs. 4 and 5). Consistently, this inserted sequence allowed FliK($\Delta 2-99 + \Delta 206-265 + I304pBPA$) to form a photo-crosslinked product with FlhB_C in a way similar to FliK(I304pBPA) (Fig. 4e). Therefore, we suggest that the inserted sequence of the suppressor mutant significantly increases the binding affinity of the core domain of FliK_C for FlhB_C. Although FliK($\Delta 2-99$) is not secreted via the flagellar type III protein export apparatus during hook assembly, it retains the ability to catalyze the substrate specificity switching of the flagellar type III protein export apparatus to a considerable degree⁴⁹. Therefore, we suggest that FliK_L is also required for efficient interaction between the core domain of FliK_C and FlhB_C. When the length of FliK_L was shortened by deletions, the export switching activity of FliK_C was reduced depending on the size of deletions (Fig. 3). Furthermore, when the linker length became longer by 40 amino-acids compared to the wild-type length, the switching function of FliK_C became worse (Fig. 6). Therefore, we propose that a proper length of FliK_L between FliK_N and FliK_C may be important for FliK_C to bind to FlhB_C to switch the substrate specificity of the flagellar type III protein export apparatus. Assuming that FliK_N suppresses the switching activity of FliK_C when FliK_N gets close to FliK_C via deletion of residues in FliK_L, it is also possible that FliK_L may push FliK_N away from FliK_C to allow these two domains to fully exert their own functions.

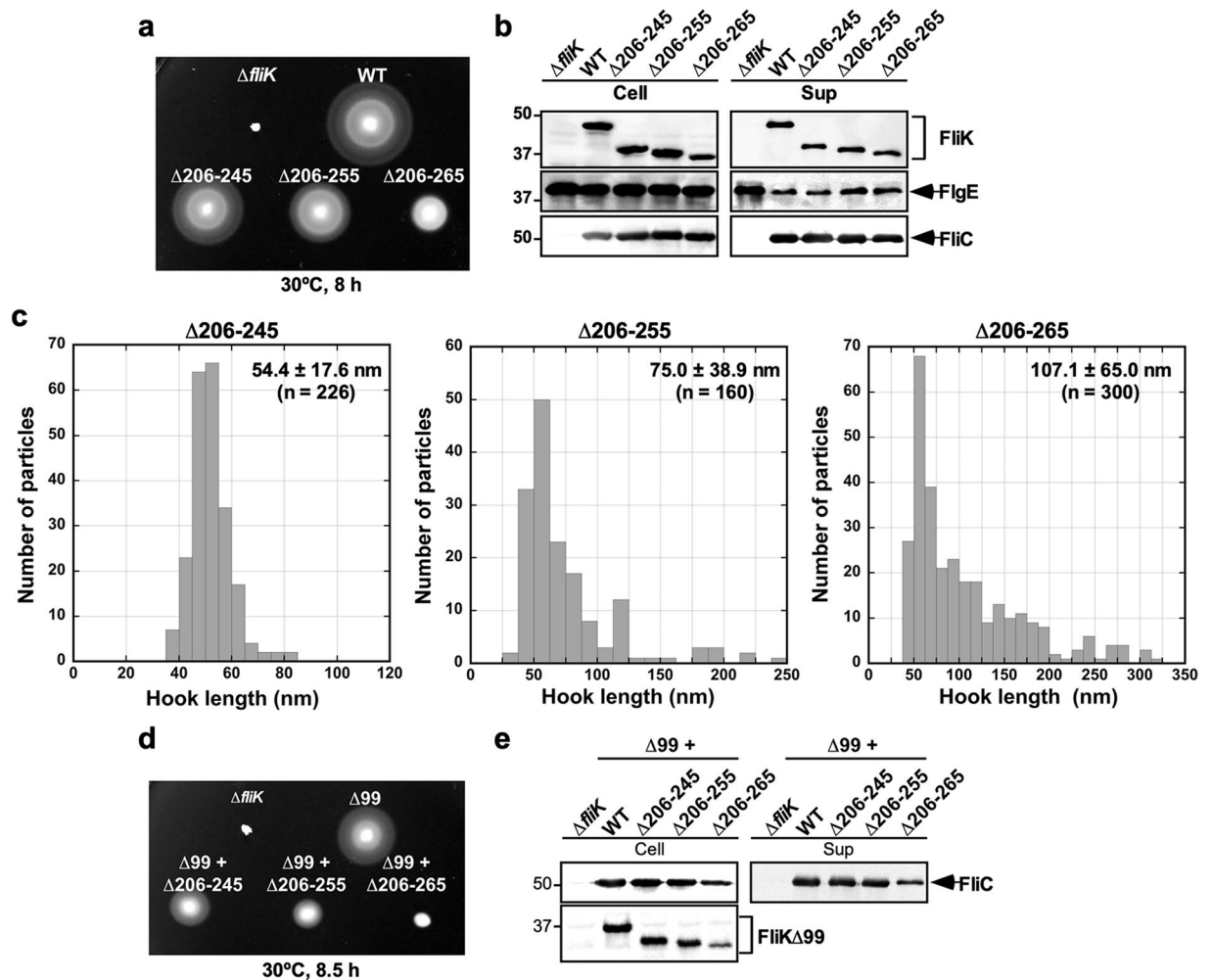


Figure 3. Effect of deletion of residues 206–245, 206–255 or 206–265 on FliK function. **(a)** Motility of TH8426 ($\Delta fliK$), SJW1103 (WT), MMK1013 ($\Delta 206-245$), MMK1014 ($\Delta 206-255$) and MMK1015 ($\Delta 206-265$) in 0.35% soft agar. Plates were incubated at 30°C for 8 hours. **(b)** Secretion assays of FliK, FlgE and FliC. Immunoblotting using polyclonal anti-FliK (1st row), anti-FlgE (2nd row) or anti-FliC (3rd row) antibody, of whole cell proteins (Cell) and culture supernatants (Sup) from the above strains. The regions of interest were cropped from original immunoblots shown in Fig. S7a in the Supplemental information using Photoshop CS6, and then the contrast and brightness were adjusted. The positions of molecular mass markers (kDa) are indicated on the left. **(c)** Histograms of hook length distribution of MMK1013 ($\Delta 206-245$), MMK1014 ($\Delta 206-255$) and MMK1015 ($\Delta 206-265$). **(d)** Motility of TH8426 harboring pTrc99AFF4 ($\Delta fliK$), pNM201 ($\Delta 99$), pMMK1028 ($\Delta 99 + \Delta 206-245$), pMMK1029 ($\Delta 99 + \Delta 206-255$) or pMMK1030 ($\Delta 99 + \Delta 206-265$) in 0.35% soft agar containing 1 mM IPTG. Plates were incubated at 30°C for 8 hours. **(e)** Secretion assay of FliC. Immunoblotting using polyclonal anti-FliC (1st row) or anti-FliK (2nd row) antibody, of whole cell proteins (Cell) and culture supernatants (Sup) from the above strains. The regions of interest were cropped from original immunoblots shown in Fig. S7b in the Supplemental information using Photoshop CS6, and then the contrast and brightness were adjusted. The positions of molecular mass markers (kDa) are indicated on the left.

The core domain of FliK_C consists of four β -strands, $\beta 1$, $\beta 2$, $\beta 3$ and $\beta 4$ and two α -helices, $\alpha 1$ and $\alpha 2$. Three parallel $\beta 1$, $\beta 3$ and $\beta 4$ strands and one anti-parallel $\beta 2$ strand form a hydrophobic core with the $\alpha 1$ and $\alpha 2$ helices (Fig. 4d)⁴⁶. Highly conserved Val-302 and Ile-304 residues in the $\beta 2$ strand, which are critical for the switching function of FliK⁴⁷, form hydrophobic interaction networks in FliK_C⁴⁶. Photo-crosslinking experiments have shown that Val-302 and Ile-304 are in very close proximity to FlhB_C, suggesting that these two residues are exposed on the molecular surface of FliK_C upon binding to FlhB_C⁴⁵. Since FliK($\Delta 2-99 + \Delta 206-265$ SP + I304pBPA) formed a photo-crosslinked product with FlhB_C whereas neither FliK($\Delta 2-99 + I304$ pBPA) nor FliK($\Delta 2-99 + \Delta 206-265 + I304$ pBPA) did (Fig. 4e), this suggests that the inserted sequence of the suppressor mutant induces a conformational change of the N-terminal portion of the core domain of FliK_C to allow Ile-304 to bind to FlhB_C. Therefore, we propose that FliK_L may be required for efficient conformational rearrangements of FliK_C to interact with FlhB_C. However, it is also possible that deletion of residues 206–265 makes FliK_N very close to FliK_C to suppress the interaction of FliK_C with FlhB_C and that the inserted sequence of the suppressor mutant may push FliK_N away from FliK_C, allowing FliK to bind to FlhB_C.

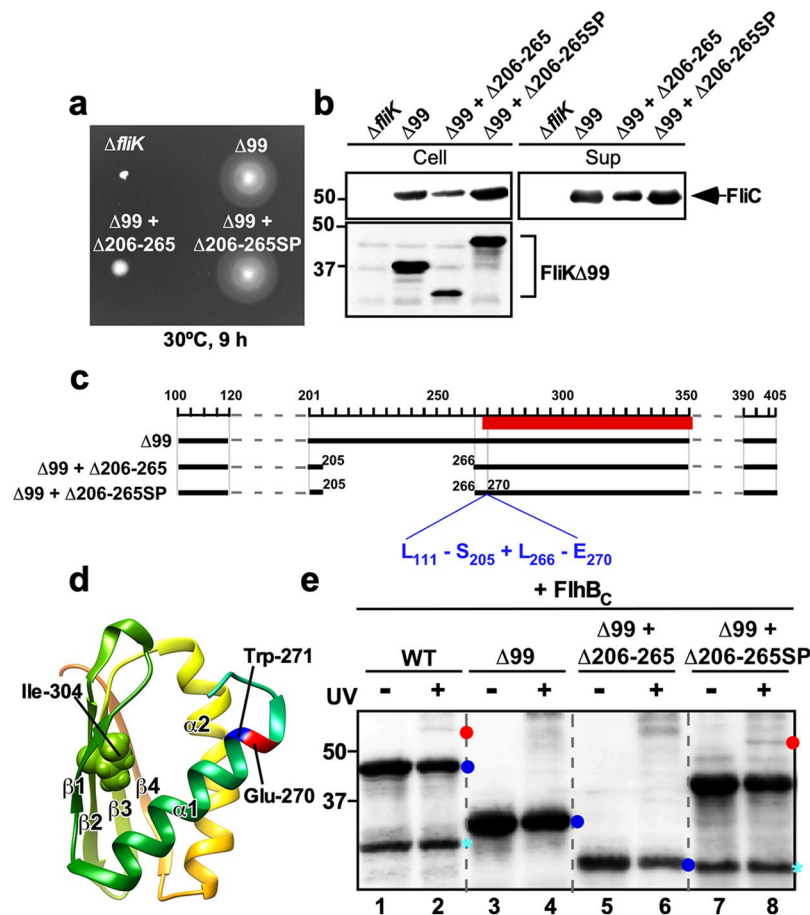


Figure 4. Isolation of pseudorevertants from the *fliK*($\Delta 99 + \Delta 206-265$) mutant. **(a)** Motility of TH8426 transformed with pTrc99A ($\Delta fliK$), pNM201 ($\Delta 99$), pMMK1030 ($\Delta 99 + \Delta 206-265$) or pMMK1030SP ($\Delta 99 + \Delta 206-265SP$) in 0.35% soft agar containing 1 mM IPTG. Plates were incubated at 30°C for 9 hours. **(b)** Secretion assay of FliC. Immunoblotting using polyclonal anti-FliC (1st row) or anti-FliK (2nd row) antibody, of whole cell proteins (Cell) and culture supernatants (Sup) prepared from the above strains. The regions of interest were cropped from original immunoblots shown in Fig. S8a in the Supplemental information using Photoshop CS6, and then the contrast and brightness were adjusted. The positions of molecular mass markers (kDa) are indicated on the left. **(c)** Location of the intragenic suppressor insertion mutation on FliK($\Delta 99 + \Delta 206-265$) and schematic bar diagram representations of FliK $\Delta 99$ products caused by a deletion of residues 206–265 and the intragenic suppressor insertion of residues 111–270 lacking residues 206–265 (L₁₁₁-S₂₀₅+L₂₆₆-E₂₇₀) between Glu-270 and Trp-271 residues. Red bar indicates a core domain of FliK_C. **(d)** NMR structure of a core domain of FliK_C (PDB ID: 2RR1). The C α backbone is color-coded from green to orange, going through the rainbow colors from the N- to the C-terminus. A highly conserved Ile-304 residue is involved in the interaction with FlhB. The inserted suppressor sequence is located between Glu-270 and Trp-271 residues. **(e)** Photo-crosslinking between FliK($\Delta 2-99$) and FlhB_C. *E. coli* BL21(DE3) cells co-expressing FliK(I304pBPA), FliK($\Delta 99 + I304pBPA$), FliK($\Delta 99 + \Delta 206-265 + I304pBPA$) or FliK($\Delta 99 + \Delta 206-265SP + I304pBPA$) with FlhB_C were UV-irradiated for 5 min (+) or not irradiated (-), and then analyzed by immunoblotting with polyclonal anti-FliK antibody. The regions of interest were cropped from original immunoblots shown in Fig. S8b in the Supplemental information using Photoshop CS6, and then the contrast and brightness were adjusted. The positions of molecular mass markers (kDa) are indicated on the left. The positions of free FliK and FliK-FlhB_C photo-crosslinked products are shown by blue and red balls, respectively. C-terminal truncated variants of FliK are shown by cyan asterisk.

FliK_C associates with and dissociates from FliK_N in solution⁴¹. When FliK_L adopts a fully extended conformation, the N-terminal portion of the core domain of FliK_C becomes disordered⁴¹. Because the length of the most extended polypeptide is 0.37 nm per residue, the stretch of FliK sequence inside the channel of the hook-basal body must be longer than 250 residues to measure the hook length of about 55 nm together with the rod length of 35 nm. Therefore, we propose that FliK_L may adopt a fully extended conformation when the hook length reaches about 55 nm, allowing Val-302 and Ile-304 in the hydrophobic core domain of FliK_C to be in very close proximity to FlhB_C to catalyze substrate specificity switching of the flagellar type III protein export apparatus.

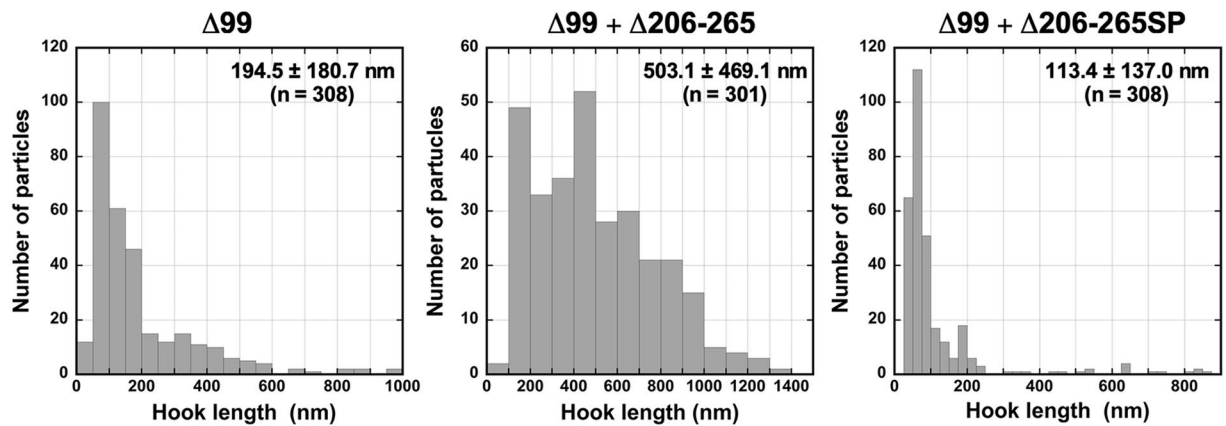


Figure 5. Effects of deletion of residues 206–265 and its intragenic suppressor insertion mutation on length distribution of the hooks produced by the *fliK*($\Delta 2-99$) mutant. Histograms of hook length distribution of TH8426 harboring pNM201 ($\Delta 99$), pMMK1030 ($\Delta 99 + \Delta 206-265$) or pMMK1030SP ($\Delta 99 + \Delta 206-265SP$).

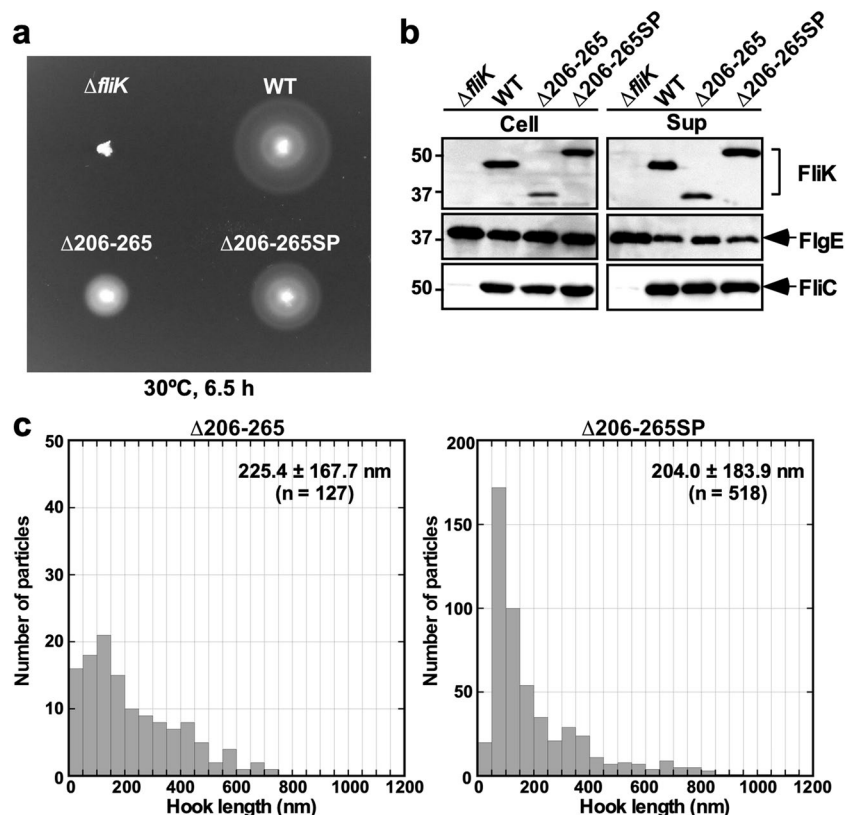


Figure 6. Effects of the inserted sequence of the intragenic *fliK*($\Delta 2-99 + \Delta 206-265$) suppressor mutant on length distribution of the hooks produced by the *fliK*($\Delta 206-265$) mutant. (a) Motility of TH8426 harboring pTrc99A ($\Delta fliK$), pKM002 (WT), pMMK1015 ($\Delta 206-265$) or pMMK1015SP ($\Delta 206-265SP$) in 0.35% soft agar. Plates were incubated at 30 °C for 6.5 hours. (b) Secretion assays of FlgE and FliC. Immunoblotting using polyclonal anti-FliK (1st row), anti-FlgE (2nd row) or anti-FliC (3rd row) antibody, of whole cell proteins (Cell) and culture supernatants (Sup) prepared from the above strains. The regions of interest were cropped from original immunoblots shown in Fig. S9 using Photoshop CS6, and then the contrast and brightness were adjusted. The positions of molecular mass markers (kDa) are indicated on the left. (c) Histograms of hook length distribution of TH8426 harboring pMMK1015 or pMMK1015SP.

Methods

Bacterial strains, plasmids and media. Bacterial strains and plasmids used in this study are listed in Table 1. To construct the *Salmonella fliK*($\Delta 206-235$), *fliK*($\Delta 206-245$), *fliK*($\Delta 206-255$) and *fliK*($\Delta 206-265$) mutant strains, the *fliK* gene on the chromosome was replaced by the *fliK*($\Delta 206-235$), *fliK*($\Delta 206-245$), *fliK*($\Delta 206-255$)

and *fliK*(Δ 206–265) alleles, using the λ Red homologous recombination system⁵⁶. L-broth contained 10 g of Bacto-Tryptone, 5 g of yeast extract and 5 g of NaCl per liter. Soft agar plates contained 10 g of Bacto Tryptone, 5 g of NaCl and 0.35% Bacto-Agar per liter. Ampicillin was added at a final concentration of 100 μ g/ml if necessary.

DNA manipulations. DNA manipulations were carried out as described⁵⁷. A series of mutant variants of FliK with deletions within FliK₁ were generated by inverse PCR using pKM002⁴⁸ or pNM201⁴⁴ as a template. The *fliK*(Δ 206–265SP) allele were generated by overlap PCR method. All of the *fliK* deletions were confirmed by DNA sequencing. DNA sequencing reactions were carried out using BigDye v3.1 (Applied Biosystems) and then the reaction mixtures were analyzed by a 3130 Genetic Analyzer (Applied Biosystems).

Motility assays in soft agar. Fresh colonies were inoculated onto 0.35% soft tryptone agar plates and incubated at 30 °C. At least seven independent measurements were carried out.

Secretion assays. Secretion assays were performed as described previously⁵⁸. *Salmonella* cells were grown in 5 ml L-broth containing 100 μ g/ml ampicillin at 30 °C with shaking until the cell density had reached an OD₆₀₀ of ca. 1.2–1.6. 1.5 ml of each culture was transferred into a 1.5 ml Eppendorf tube. After centrifugation (15,000 g, 5 min, 4 °C), cell pellets and culture supernatants were collected, separately. The cells were resuspended in OD₆₀₀ \times 250 μ l of SDS-loading buffer (62.5 mM Tris-HCl, pH 6.8, 2% SDS, 10% glycerol, 0.001% bromophenol blue) containing 1 μ l of 2-mercaptoethanol and heated at 95 °C for 3 min. Trichloroacetic acid was added to each culture supernatant at a final concentration of 10%. After leaving on ice for 1 h, proteins in the culture supernatants were precipitated by centrifugation at 20,000 g for 20 min. Pellets were suspended in OD₆₀₀ \times 25 μ l of a Tris-SDS loading buffer (one volume of 1 M Tris, nine volumes of 1 \times SDS loading buffer) containing 1 μ l of 2-mercaptoethanol and heated at 95 °C for 3 min. After sodium dodecyl sulfate-polyacrylamide gel electrophoresis (SDS-PAGE), immunoblotting with polyclonal anti-FlgE, anti-FliC or anti-FliK antibody was carried out as described previously¹⁶. Detection was done with an ECL prime western blotting detection reagent (GE Healthcare). Chemiluminescence signals were captured by a Luminoimage analyzer LAS-3000 (GE Healthcare). The regions of interest were cropped from original immunoblots shown in the Supplemental information using a software, Photoshop CS6, and then the contrast and brightness were adjusted. At least three independent experiments were performed.

Electron microscopy. Osmotically shocked *Salmonella* cells were prepared described previously⁴⁵. After centrifugation (18,500 g, 30 min), the cell pellets were resuspended in 200 μ l of H₂O. Samples were applied to carbon-coated copper grids and were negatively stained with 1.0% (W/V) phosphotungstic acid, pH 7.0. Micrographs were recorded at a magnification of \times 5,000 with a JEM-1200EXII transmission electron microscope (JEOL, Tokyo, Japan) operating at 80 kV.

Hook-basal bodies and polyhook-basal bodies were isolated as described before²⁷. *Salmonella* cells were grown in 5 l L-broth containing ampicillin at 30 °C with shaking until the cell density had reached an OD₆₀₀ of ca. 1.0. The cells were harvested by centrifugation (10,000 g, 10 min, 4 °C) and suspended in 20 ml of ice-cold 0.1 M Tris-HCl pH 8.0, 0.5 M sucrose, followed by addition of EDTA and lysozyme at the final concentrations of 10 mM and 0.1 mg/ml, respectively. The cell suspensions were stirred for 30 min at 4 °C and then were solubilized on ice for 1 hour by adding Triton X-100 and MgSO₄ at final concentrations of 1% and 10 mM, respectively. The cell lysates were adjusted to pH 10.5 with 5 M NaOH and then centrifuged (10,000 g, 20 min, 4 °C) to remove cell debris. After ultracentrifugation (45,000 g, 60 min, 4 °C), pellets were resuspended in 10 mM Tris-HCl, pH 8.0, 5 mM EDTA, 1% Triton X-100, and the solution was loaded a 20–50% (w/w) sucrose density gradient in 10 mM Tris-HCl, pH 8.0, 5 mM EDTA, 1% Triton X-100. After ultracentrifugation (49,100 g, 13 h, 4 °C), intact flagella were collected and ultracentrifuged (60,000 g, 60 min, 4 °C). Pellets were suspended in 50 mM glycine, pH 2.5, 0.1% Triton X100, and were incubated at room temperature for 30 min to depolymerize flagellar filaments. After ultracentrifugation (60,000 g, 60 min, 4 °C), pellets were resuspended in 50 μ l of 10 mM Tris-HCl, pH 8.0, 5 mM EDTA, 0.1% Triton X100. Samples were negatively stained with 2% (w/v) uranyl acetate. Samples were applied to carbon-coated copper grids and were negatively stained with 2% (w/v) uranyl acetate. Electron micrographs were recorded with a JEM-1011 transmission electron microscope (JEOL, Tokyo, Japan) operated at 100 kV and equipped with a F415 CCD camera (TVIPS, Gauting, Germany). Hook length was measured by ImageJ version 1.48 (National Institutes of Health).

Photo-crosslinking. *E. coli* BL21(DE3) cells harboring pEVOL⁵⁹ and a pETDuet-based plasmid encoding both FliK with an amber mutation and FlhB_C were exponentially grown at 30 °C in L-broth containing 1 mM pBPA. Then, 100 μ M IPTG and 0.02% arabinose were added and the incubation was continued until the culture density had reached an OD₆₀₀ of ca. 1.4–1.5. Photo-crosslinking was carried out as described previously⁶⁰. The cell pellets were harvested by centrifugation, suspended in SDS-loading buffer, and heated at 95 °C for 3 min. After SDS-PAGE, immunoblotting with polyclonal anti-FliK antibody was carried out. Detection was done with an ECL prime western blotting detection reagent. Chemiluminescence signals were captured by a Luminoimage analyzer LAS-3000. The regions of interest were cropped from original immunoblots shown in the Supplemental information using a software, Photoshop CS6, and then the contrast and brightness were adjusted. At least three independent experiments were performed.

Data availability

All data generated or analyzed during this study are included in this published article and its Supplementary Information files.

Received: 25 March 2019; Accepted: 2 January 2020;

Published online: 21 January 2020

References

- Nakamura, S. & Minamino, T. Flagella-driven motility of bacteria. *Biomolecules*. **9**, 279 (2019).
- Hirano, T., Yamaguchi, S., Oosawa, K. & Aizawa, S.-I. Roles of FliK and FlhB in determination of flagellar hook length in *Salmonella typhimurium*. *J. Bacteriol.* **176**, 5439–5449 (1994).
- Spöring, I. *et al.* Hook length of the bacterial flagellum is optimized for maximal stability of the flagellar bundle. *PLOS Biol.* **16**, e2006989 (2018).
- Minamino, T. Protein export through the bacterial flagellar type III export pathway. *Biochim. Biophys. Acta.* **1843**, 1642–1648 (2014).
- Ohnishi, K., Ohto, Y., Aizawa, S., Macnab, R. M. & Iino, T. FlgD is a scaffolding protein needed for flagellar hook assembly in *Salmonella typhimurium*. *J. Bacteriol.* **176**, 2272–2281 (1994).
- Moriya, N., Minamino, T., Imada, K. & Namba, K. Genetic analysis of the bacterial hook-capping protein FlgD responsible for hook assembly. *Microbiology* **157**, 1354–1362 (2011).
- Sakai, T., Inoue, Y., Terahara, N., Namba, K. & Minamino, T. A triangular loop of domain D1 of FlgE is essential for hook assembly but not for the mechanical function. *Biochem. Biophys. Res. Commun.* **495**, 1789–1794 (2018).
- Ferris, H. U. & Minamino, T. Flipping the switch: bringing order to flagellar assembly. *Trends Microbiol.* **14**, 519–526 (2006).
- Minamino, T., Imada, K. & Namba, K. Mechanisms of type III protein export for bacterial flagellar assembly. *Mol. Biosyst.* **4**, 1105–1115 (2008).
- Minamino, T. Hierarchical protein export mechanism of the bacterial flagellar type III protein export apparatus. *FEMS Microbiol. Lett.* **365**, fny117 (2018).
- Kutsukake, K., Minamino, T. & Yokoseki, T. Isolation and characterization of FliK-independent flagellation mutants from *Salmonella typhimurium*. *J. Bacteriol.* **176**, 7625–7629 (1994).
- Williams, A. W. *et al.* Mutations in fliK and flhB affecting flagellar hook and filament assembly in *Salmonella typhimurium*. *J. Bacteriol.* **178**, 2960–2970 (1996).
- Kutsukake, K. Hook-length control of the export-switching machinery involves a double-locked gate in *Salmonella typhimurium* flagellar morphogenesis. *J. Bacteriol.* **179**, 1268–1273 (1997).
- Hirano, T., Mizuno, S., Aizawa, S.-I. & Hughes, K. T. Mutations in Flk, FlgG, FlhA, and FlhE that affect the flagellar type III secretion specificity switch in *Salmonella enterica*. *J. Bacteriol.* **181**, 3938–3949 (2009).
- Minamino, T., Iino, T. & Kutsukake, K. Molecular characterization of the *Salmonella typhimurium* flhB operon and its protein products. *J. Bacteriol.* **176**, 7630–7637 (1994).
- Minamino, T. & Macnab, R. M. Components of the *Salmonella* flagellar export apparatus and classification of export substrates. *J. Bacteriol.* **181**, 1388–1394 (1999).
- Abrusci, P. *et al.* Architecture of the major component of the type III secretion system export apparatus. *Nat. Struct. Mol. Biol.* **20**, 99–104 (2013).
- Terahara, N. *et al.* Insight into structural remodeling of the FlhA ring responsible for bacterial flagellar type III protein export. *Sci. Adv.* **4**, eaao7054 (2018).
- Minamino, T. & Macnab, R. M. Interactions among components of the *Salmonella* flagellar export apparatus and its substrates. *Mol. Microbiol.* **35**, 1052–1064 (2000).
- Minamino, T. *et al.* Role of the C-terminal cytoplasmic domain of FlhA in bacterial flagellar type III protein export. *J. Bacteriol.* **192**, 1929–1936 (2010).
- Minamino, T., Morimoto, Y. V., Hara, N. & Namba, K. An energy transduction mechanism used in bacterial flagellar type III protein export. *Nat. Commun.* **2**, 475 (2011).
- Bange, G. *et al.* FlhA provides the adaptor for coordinated delivery of late flagella building blocks to the type III secretion system. *Proc. Natl. Acad. Sci. USA* **107**, 11295–11300 (2010).
- Minamino, T. *et al.* Interaction of a bacterial flagellar chaperone FlgN with FlhA is required for efficient export of its cognate substrates. *Mol. Microbiol.* **83**, 775–788 (2012).
- Kinoshita, M., Hara, N., Imada, K., Namba, K. & Minamino, T. Interactions of bacterial chaperone-substrate complexes with FlhA contribute to co-ordinating assembly of the flagellar filament. *Mol. Microbiol.* **90**, 1249–1261 (2013).
- Xing, Q. *et al.* Structure of chaperone-substrate complexes docked onto the export gate in a type III secretion system. *Nat. Commun.* **9**, 1773.
- Minamino, T. *et al.* FliH and FliI ensure efficient energy coupling of flagellar type III protein export in *Salmonella*. *MicrobiologyOpen* **5**, 424–435 (2016).
- Inoue, Y., Morimoto, Y. V., Namba, K. & Minamino, T. Novel insights into the mechanism of well-ordered assembly of bacterial flagellar proteins in *Salmonella*. *Sci. Rep.* **8**, 1787 (2018).
- Minamino, T. & Macnab, R. M. Domain structure of *Salmonella* FlhB, a flagellar export component responsible for substrate specificity switching. *J. Bacteriol.* **182**, 4906–4919 (2000).
- Fraser, G. M. *et al.* Substrate specificity of type III flagellar protein export in *Salmonella* is controlled by subdomain interactions in FlhB. *Mol. Microbiol.* **48**, 1043–1057 (2003).
- Ferris, H. U. *et al.* FlhB regulates ordered export of flagellar components via autocleavage mechanism. *J. Biol. Chem.* **280**, 41236–41242 (2005).
- Evans, L. D., Poulter, S., Terentjev, E. M., Hughes, C. & Fraser, G. M. A chain mechanism for flagellum growth. *Nature* **504**, 287–290 (2013).
- McMurry, J. L. *et al.* Weak interactions between *Salmonella enterica* FlhB and other flagellar export apparatus proteins govern type III secretion dynamics. *PLOS One* **10**, e0134884 (2015).
- Inoue, Y. *et al.* Structural insight into the substrate specificity switch mechanism of the type III protein export apparatus. *Structure* **27**, 965–976 (2019).
- Aldridge, P., Karlinsey, J. E., Becker, E., Chevance, F. F. & Hughes, K. T. Flk prevents premature secretion of the anti sigma factor FlgM into the preplasm. *Mol. Microbiol.* **60**, 630–642 (2006).
- Minamino, T., González-Pedrajo, B., Yamaguchi, K., Aizawa, S.-I. & Macnab, R. M. FliK, the protein responsible for flagellar hook length control in *Salmonella*, is exported during hook assembly. *Mol. Microbiol.* **34**, 295–304 (1999).
- Erhardt, M. *et al.* The role of the FliK molecular ruler in hook-length control in *Salmonella enterica*. *Mol. Microbiol.* **75**, 1272–1284 (2010).
- Erhardt, M., Singer, H. M., Wee, D. H., Keener, J. P. & Hughes, K. T. An infrequent molecular ruler controls flagellar hook length in *Salmonella enterica*. *EMBO J.* **30**, 2948–2961 (2011).
- Uchida, K. & Aizawa, S.-I. The flagellar soluble protein FliK determines the minimal length of the hook in *Salmonella enterica* serovar Typhimurium. *J. Bacteriol.* **196**, 1753–1758 (2014).
- Kawagishi, I., Homma, M., Williams, A. W. & Macnab, R. M. Characterization of the flagellar hook length control protein of *Salmonella typhimurium* and *Escherichia coli*. *J. Bacteriol.* **178**, 2954–2959 (1996).
- Minamino, T. *et al.* Domain organization and function of *Salmonella* FliK, a flagellar hook-length control protein. *J. Mol. Biol.* **341**, 491–502 (2004).
- Kodera, N., Uchida, K., Ando, T. & Aizawa, S.-I. Two-ball structure of the flagellar hook-length control protein FliK as revealed by high-speed atomic force microscopy. *J. Mol. Biol.* **427**, 406–414 (2015).
- Shibata, S. *et al.* FliK regulates flagellar hook length as an internal ruler. *Mol. Microbiol.* **64**, 1404–1415 (2007).

43. Moriya, N., Minamino, T., Hughes, K. T., Macnab, R. M. & Namba, K. The type III flagellar export specificity switch is dependent on FliK ruler and a molecular clock. *J. Mol. Biol.* **359**, 466–477 (2006).
44. Minamino, T., Moriya, N., Hirano, T., Hughes, K. T. & Namba, K. Interaction of FliK with the bacterial flagellar hook is required for efficient export specificity switching. *Mol. Microbiol.* **74**, 239–251 (2009).
45. Kinoshita, M., Aizawa, S.-I., Inoue, Y., Namba, K. & Minamino, T. The role of intrinsically disordered C-terminal region of FliK in substrate specificity switching of the bacterial flagellar type III export apparatus. *Mol. Microbiol.* **105**, 572–588 (2017).
46. Mizuno, S., Amida, H., Kobayashi, N., Aizawa, S.-I. & Tate, S. The NMR structure of FliK, the trigger for the switch of substrate specificity in the flagellar type III secretion apparatus. *J. Mol. Biol.* **409**, 558–573 (2011).
47. Minamino, T., Ferris, H. U., Morioya, N., Kihara, M. & Namba, K. Two parts of the T3S4 domain of the hook-length control protein FliK are essential for the substrate specificity switching of the flagellar type III export apparatus. *J. Mol. Biol.* **362**, 1148–1158 (2006).
48. Muramoto, K., Makishima, S., Aizawa, S.-I. & Macnab, R. M. Effect of cellular level of FliK on flagellar hook and filament assembly in *Salmonella typhimurium*. *J. Mol. Biol.* **277**, 871–882 (1998).
49. Hirano, T., Shibata, S., Ohnishi, K., Tani, T. & Aizawa, S. N-terminal signal region of FliK is dispensable for length control of the flagellar hook. *Mol. Microbiol.* **56**, 346–360 (2005).
50. Kubori, T. *et al.* Supramolecular structure of the *Salmonella typhimurium* type III protein secretion system. *Science* **280**, 602–605 (1998).
51. Journet, L., Agrain, C., Broz, P. & Cornelis, G. R. The needle length of bacterial injectisomes is determined by a molecular ruler. *Science* **302**, 1757–1760 (2003).
52. Wee, D. H. & Hughes, K. T. Molecular ruler determines needle length for the *Salmonella* Spi-1 injectisome. *Proc. Natl. Acad. Sci. USA* **112**, 4098–103 (2015).
53. Agrain, C. *et al.* Characterization of a type III secretion substrate specificity switch (T3S4) domain in YscP from *Yersinia enterocolitica*. *Mol. Microbiol.* **56**, 54–67 (2005).
54. Bergeron, J. R. *et al.* The structure of a type 3 secretion system (T3SS) ruler protein suggests a molecular mechanism for needle length sensing. *J. Biol. Chem.* **291**, 1676–1691 (2016).
55. Ho, O. *et al.* Characterization of the ruler protein interaction interface on the substrate specificity switch protein in the *Yersinia* type III secretion system. *J. Biol. Chem.* **292**, 3299–3311 (2017).
56. Datsenko, K. A. & Wanner, B. L. One-step inactivation of chromosomal genes in *Escherichia coli* K-12 using PCR products. *Proc. Natl. Acad. Sci. USA* **97**, 6640–6645 (2000).
57. Saijo-Hamano, Y., Minamino, T., Macnab, R. M. & Namba, K. Structural and functional analysis of the C-terminal cytoplasmic domain of FlhA, an integral membrane component of the type III flagellar protein export apparatus in *Salmonella*. *J. Mol. Biol.* **343**, 457–466 (2004).
58. Minamino, T., Kinoshita, M. & Namba, K. Fuel of the bacterial flagellar type III protein export apparatus. *Methods Mol. Biol.* **1593**, 3–16 (2017).
59. Young, T. S., Ahmad, I., Yin, J. A. & Schultz, P. G. An enhanced system for unnatural amino acid mutagenesis in *E. coli*. *J. Mol. Biol.* **395**, 361–374 (2010).
60. Hara, N., Morimoto, Y. V., Kawamoto, A., Namba, K. & Minamino, T. Interaction of the extreme N-terminal region of FliH with FlhA is required for efficient bacterial flagellar protein export. *J. Bacteriol.* **194**, 5353–5360 (2012).
61. Yamaguchi, S., Fujita, H., Sugata, K., Taira, T. & Iino, T. Genetic analysis of H2, the structural gene for phase-2 flagellin in *Salmonella*. *J. Gen. Microbiol.* **130**, 255–265 (1984).
62. Ohnishi, K., Fan, F., Schoenhals, G. J., Kihara, M. & Macnab, R. M. The FliO, FliP, FliQ, and FliR proteins of *Salmonella typhimurium*: putative components for flagellar assembly. *J. Bacteriol.* **179**, 6092–6099 (1997).

Acknowledgements

We acknowledge Prof. P.G. Schultz for his kind gift of pEVOL. This work was supported in part by JSPS KAKENHI Grant Numbers JP18K14638 (to M.K.), JP25000013 (to K.N.), and JP26293097 and JP19H03182 (to T.M.) and MEXT KAKENHI Grant Number JP15H01640 (to T.M.). This work has also been partially supported by JEOL YOKOGUSHI Research Alliance Laboratories of Osaka University to K.N.

Author contributions

M.K., N.K., S.I.A. and T.M. conceived and designed research; M.K., S.T., Y.I., S.I.A. and T.M. performed research; M.K., S.T., Y.I., S.I.A. and T.M. analysed the data; and M.K., K.N., S.I.A. and T.M. wrote the paper based on discussion with other authors.

Competing interests

The authors declare no competing interests.

Additional information

Supplementary information is available for this paper at <https://doi.org/10.1038/s41598-020-57782-5>.

Correspondence and requests for materials should be addressed to T.M.

Reprints and permissions information is available at www.nature.com/reprints.

Publisher's note Springer Nature remains neutral with regard to jurisdictional claims in published maps and institutional affiliations.



Open Access This article is licensed under a Creative Commons Attribution 4.0 International License, which permits use, sharing, adaptation, distribution and reproduction in any medium or format, as long as you give appropriate credit to the original author(s) and the source, provide a link to the Creative Commons license, and indicate if changes were made. The images or other third party material in this article are included in the article's Creative Commons license, unless indicated otherwise in a credit line to the material. If material is not included in the article's Creative Commons license and your intended use is not permitted by statutory regulation or exceeds the permitted use, you will need to obtain permission directly from the copyright holder. To view a copy of this license, visit <http://creativecommons.org/licenses/by/4.0/>.

© The Author(s) 2020